



Cite this: *RSC Appl. Polym.*, 2024, **2**, 670

## Virus adsorption and elution using cationic polymer brushes: potential applications for passive sampling in wastewater-based epidemiology†

Junya Uchida,<sup>a</sup> Miaomiao Liu,<sup>b</sup> Shizuka Matsuyama,<sup>a</sup> Hiroyuki Katayama<sup>\*a,c</sup> and Takashi Kato<sup>†a,c,d</sup>

Wastewater-based epidemiology (WBE) has been recognized as a promising approach for rapid monitoring of infectious diseases in local communities. Development of adsorption materials that efficiently capture viruses is important in WBE to provide precise information on the prevalence of viral infections. Herein, ionic polymer brushes are synthesized for the tuning of virus adsorption and elution. Quaternary ammonium-based cationic polymer brushes exhibit higher adsorption of enveloped and nonenveloped viruses than a low-molecular-weight amine adduct. Moreover, efficient and selective elution of Aichivirus from the polymer brushes is demonstrated. These cationic polymer brushes may be useful as materials for passive sampling of viruses from water.

Received 23rd October 2023,  
Accepted 1st April 2024

DOI: 10.1039/d3lp00216k

rsc.li/rscapppolym

### Introduction

Wastewater-based epidemiology (WBE) has attracted much attention because it enables rapid monitoring of infectious diseases in local communities.<sup>1,2</sup> Effective detection of viruses from sewage and environmental water is important to provide precise information on the prevalence of viral infections.<sup>3–5</sup> For example, detection of Aichivirus (AiV), which is suggested as an appropriate indicator of viral contamination in the environment,<sup>6</sup> may be useful to assess human faecal pollution.<sup>6–9</sup> In WBE analysis, passive sampling is a virus collection method involving the placement of adsorption materials in water.<sup>10,11</sup> Commercially available materials such as cotton gauze, glass beads, and polymer membranes have been used as adsorption materials to capture viruses.<sup>12–14</sup> The tuning of the surface properties of these materials is considered to be a key to achieve efficient recovery of viruses from wastewater.<sup>14,15</sup>

Our intention is to provide a new approach for tuning virus adsorption and elution for passive sampling of viruses from water (Fig. 1). We expected that ionic polymer brushes of grafting polymers may be useful in tuning virus adsorption and elution due to their electrostatic interactions with viruses. Grafting polymers on solid substrates have been widely studied to develop stimuli-responsive functional soft surfaces.<sup>16–23</sup> For example, polyelectrolyte brushes were formed on a variety of surfaces to provide lubrication,<sup>24–26</sup> antifouling,<sup>18,27,28</sup> and antibacterial functions.<sup>29,30</sup> Thermoresponsive surfaces based on poly(*N*-isopropylacrylamide) brushes have been developed for applications as substrates to control cell adhesion and detachment.<sup>29,31,32</sup> We also reported thermoresponsive polymer brush matrices for tuning the morphologies of organic/inorganic hybrid thin films.<sup>33–35</sup> Cationic polymer brushes may exhibit higher adsorption of viruses because most viruses are reported to be negatively charged at neutral pH.<sup>36</sup> Cationic polymers and polymer hybrids have been studied for the development of virus adsorption,<sup>37</sup> virus removal membranes,<sup>38–42</sup> and antimicrobial materials.<sup>43–45</sup> The use of polymer brushes for passive sampling of viruses from sewage has not been attempted, although purification of viral vectors for gene therapy by using thermoresponsive-anionic mixed polymer brushes has been reported.<sup>46</sup>

Here we report virus adsorption and elution using ionic polymer brushes grafted on the substrates (Fig. 1). The effects of the surface properties of the modified substrates on virus adsorption and elution were examined by using cocktail solutions containing different types of viruses.

<sup>a</sup>Department of Chemistry and Biotechnology, School of Engineering, The University of Tokyo, 7-3-1 Hongo, Bunkyo-ku, Tokyo 113-8656, Japan.

E-mail: kato@chiral.t.u-tokyo.ac.jp

<sup>b</sup>Department of Urban Engineering, School of Engineering, The University of Tokyo, 7-3-1 Hongo, Bunkyo-ku, Tokyo 113-8656, Japan.

E-mail: katayama@env.t.u-tokyo.ac.jp

<sup>c</sup>Research Center for Water Environment Technology, School of Engineering, The University of Tokyo, 7-3-1 Hongo, Bunkyo-ku, Tokyo 113-8656, Japan

<sup>d</sup>Research Initiative for Supra-Materials, Shinshu University, 4-17-1 Wakasato, Nagano 380-8553, Japan

† Electronic supplementary information (ESI) available. See DOI: <https://doi.org/10.1039/d3lp00216k>



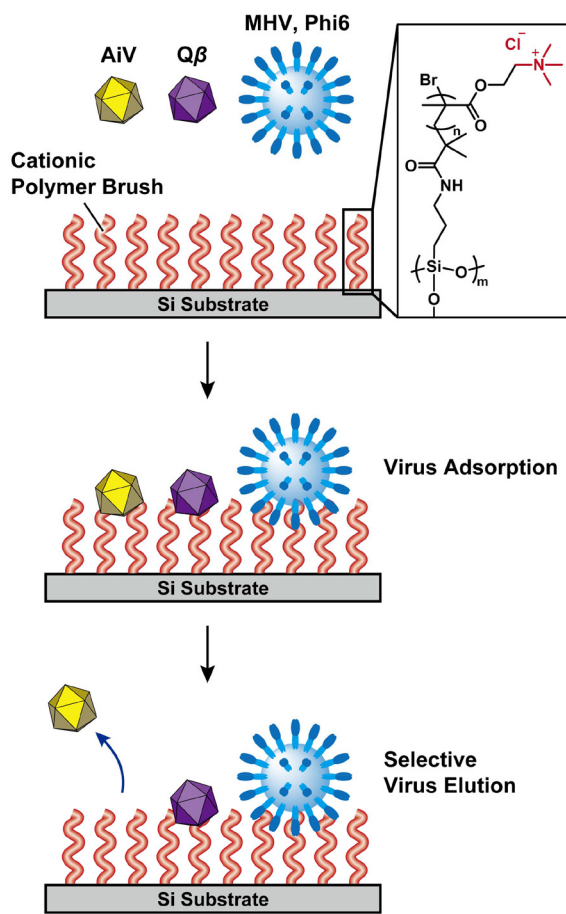


**Fig. 1** Schematic illustration of virus adsorption and elution using cationic polymer brushes grafted on a silicon substrate. AiV: Aichivirus; Q $\beta$ : F-RNA-specific bacteriophage Q $\beta$ ; MHV: murine hepatitis virus; and Phi6: *Pseudomonas syringae* phage Phi6.

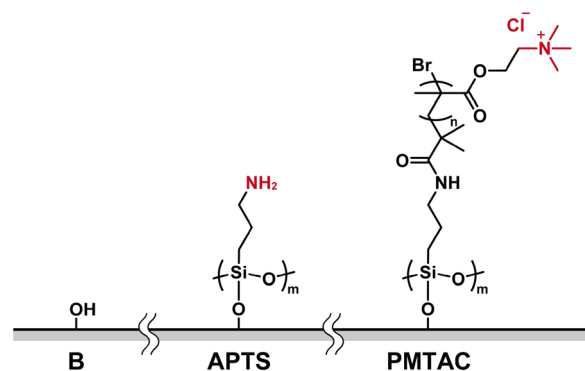


**Fig. 2** Chemical structures of the surfaces of the silicon substrates. **B**: bare substrates; **APTS**: 3-aminopropyltriethoxysilane (APTS)-functionalized substrates; and **PMTAC**: poly[2-(methacryloyloxy)ethyltrimethylammonium chloride] (PMTAC)-grafted substrates.

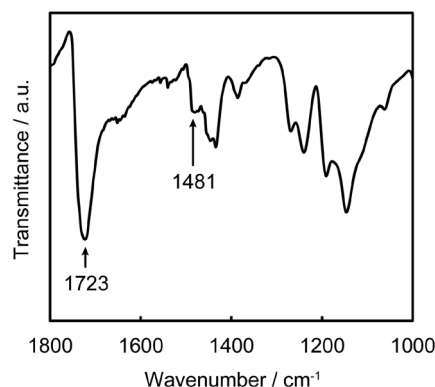


**Fig. 3** FT-IR spectrum of the poly[2-(methacryloyloxy)ethyltrimethylammonium chloride] (PMTAC) brush.

## Results and discussion

### Materials design and synthesis

Ionic polymer brushes consisting of poly[2-(methacryloyloxy)ethyltrimethylammonium chloride] (PMTAC) (Fig. 2) were synthesized by surface-initiated atom transfer radical polymerization (ATRP) (Fig. S1†).<sup>47–49</sup> An ATRP initiator, 2-bromo-2-methyl-*N*-(3-(triethoxysilyl)propyl)propanamide, was immobilized on a silicon substrate. This substrate was used for surface-initiated ATRP to obtain the PMTAC-grafted substrates. In addition, silicon substrates modified with 3-aminopropyltriethoxysilane (APTS) (Fig. 2) were prepared as a control material containing a low-molecular-weight amine branch. The PMTAC-grafted substrates (**PMTAC**) and APTS-functionalized substrates (**APTS**) as well as nonmodified bare silicon substrates (**B**) were used to examine virus adsorption and elution.

### Structures of the PMTAC-grafted surface

The formation of the PMTAC brushes grafted on the substrates was examined (Fig. 3, 4, Table 1, Fig. S2 and S3†). Fig. 3 shows

a Fourier-transform infrared (FT-IR) spectrum of a silicon substrate that underwent surface-initiated ATRP. A strong absorption peak corresponding to the C=O stretching vibration of the PMTAC brushes was observed at 1723 cm<sup>−1</sup>.<sup>50,51</sup> In addition, the surface exhibited an absorption band around 1481 cm<sup>−1</sup>. This can be assigned to a vibration of the quaternary ammonium group of the PMTAC brushes.<sup>50,51</sup> These results show that the surface-initiated ATRP led to the preparation of the cationic polymer brushes consisting of PMTAC.

The surface morphology of **PMTAC** was observed by atomic force microscopy (AFM) (Fig. 4a). The surface of **PMTAC** was sufficiently covered with the polymer brushes (Fig. 4a), while those of **APTS** (Fig. 4b), **B** (Fig. 4c), and the ATRP initiator-modified (Fig. S3†) substrates were smoother. Based on these observations, the PMTAC brushes are expected to efficiently interact with viruses to provide higher virus adsorption.

The surface wettability of **PMTAC** was examined by contact angle measurements (Table 1). The water contact angle of **PMTAC** was larger than those of **APTS** and **B** (Table 1). It was reported that surface wettability was affected by the nanostructures of the surface.<sup>52</sup> The uneven surface of **PMTAC** (Fig. 4a) may result in the formation of a more hydrophobic



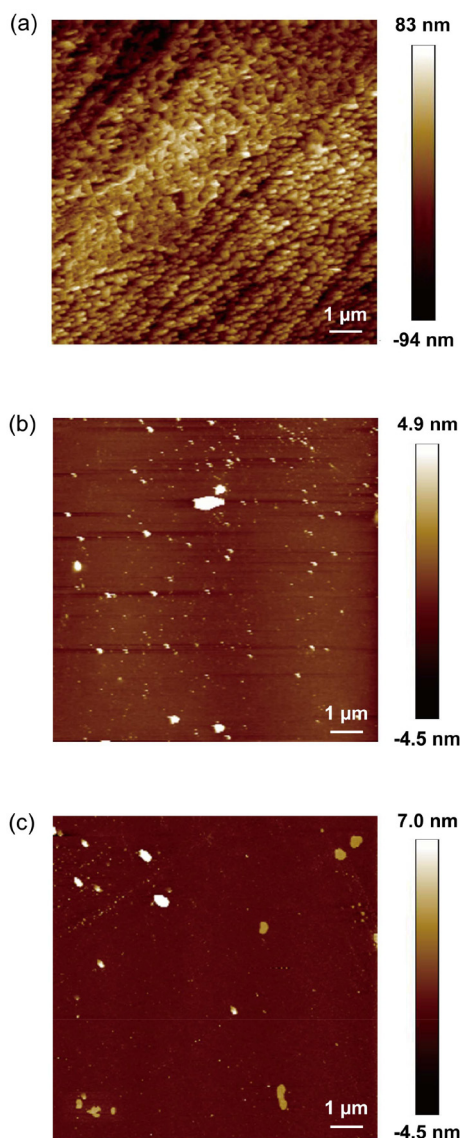


Fig. 4 AFM images of (a) the poly[2-(methacryloyloxy)ethyltrimethylammonium chloride] (PMTAC)-grafted, (b) 3-aminopropyltriethoxysilane (APTS)-functionalized, and (c) nonmodified bare substrates.

Table 1 Surface properties of the bare and modified substrates

Materials <sup>a</sup>	Contact angle (degree)	Solvent-accessible cations <sup>b</sup> ( $10^{15} \text{ cm}^{-2}$ )
<b>B</b>	$36 \pm 2.3$	$0.0 \pm 0.0$
<b>APTS</b>	$50 \pm 2.2$	$0.0 \pm 0.0$
<b>PMTAC</b>	$69 \pm 12$	$1.1 \pm 0.4$

<sup>a</sup> **B**: bare substrates; **APTS**: 3-aminopropyltriethoxysilane (APTS)-functionalized substrates; and **PMTAC**: poly[2-(methacryloyloxy)ethyltrimethylammonium chloride] (PMTAC)-grafted substrates. <sup>b</sup> The number of solvent-accessible cations was estimated with the fluorescein adsorption assay.<sup>53,54</sup>

surface than those of **APTS** and **B**. The substrates modified with the ATRP initiator also formed a hydrophobic surface with a contact angle of  $86 \pm 1.5^\circ$ .

To gain further insights into the surface properties, the number of solvent-accessible cations on the surfaces was estimated (Table 1). A fluorescein adsorption assay<sup>53,54</sup> was performed for **PMTAC**, **APTS**, and **B**. The charge density of **PMTAC** was estimated to be about  $10^{15}$  cations per  $\text{cm}^2$  (Table 1). For **APTS** and **B**, no significant differences in the number of solvent-accessible cations were observed, although the contact angle of these substrates was different. The higher charge density of **PMTAC** may be useful for efficient adsorption of viruses.

### Adsorption and elution of viruses

In the adsorption and elution experiments, four types of viruses including **AiV**, F-RNA-specific bacteriophage **Q $\beta$** , *Pseudomonas syringae* phage **Phi6**, and murine hepatitis virus (MHV) were employed to represent different virus types in wastewater. **AiV** and **Q $\beta$**  are nonenveloped viruses, while MHV and **Phi6** are enveloped viruses. The sizes of **AiV** and **Q $\beta$**  were reported to be around 30 nm,<sup>55–57</sup> while those of MHV and **Phi6** were reported to be approximately 80 nm.<sup>58,59</sup> These nonenveloped and enveloped viruses were mixed in 100 mM phosphate buffered saline (PBS) to prepare feed solutions (referred to as Feed). To assess the virus adsorption, the feed solutions were placed on the surface-modified and bare silicon substrates for 5 h, followed by washing the substrates with PBS to collect the solution (referred to as Permeate). The elution of the viruses from the substrates was performed with sterile beef

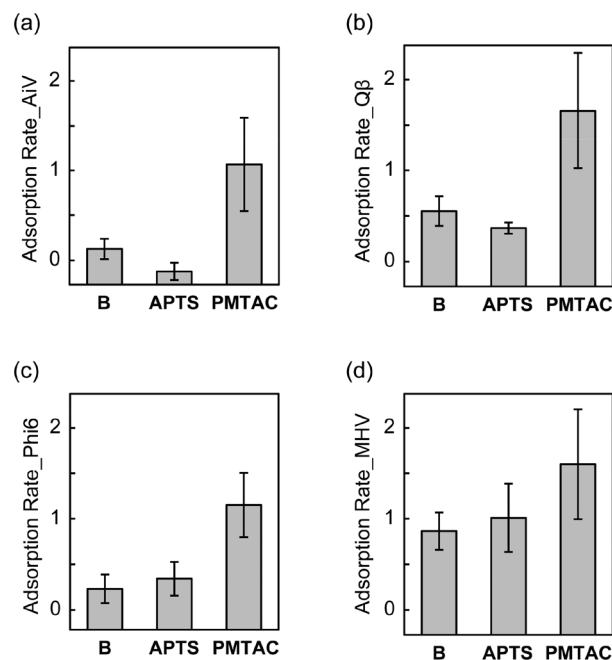


Fig. 5 Adsorption rates of (a) **AiV**, (b) **Q $\beta$** , (c) **Phi6**, and (d) MHV by the silicon-based substrates. Adsorption rate ( $\log_{10} \text{Ads}$ ) =  $\log_{10}(\text{virus in Feed}/\text{virus in Permeate})$ . **B**: bare substrates ( $n = 8$ ); **APTS**: the 3-aminopropyltriethoxysilane (APTS)-functionalized substrates ( $n = 4$ ); and **PMTAC**: the poly[2-(methacryloyloxy)ethyltrimethylammonium chloride] (PMTAC)-grafted substrates ( $n = 10$ ).



extract (3%, pH = 9), which is generally used for virus elution.<sup>15,60</sup> After soaking the substrates in the beef extract for 1 h, the solution was collected as an eluate (referred to as Eluate). The concentrations of the four viruses in the Feed, Permeate, and Eluate were quantified with reverse transcription quantitative polymerase chain reaction (RT-qPCR) to estimate the virus adsorption and elution rates. Adsorption was quantified by calculating the logarithmic removal from the

Feed to the Permeate (eqn (1)) whereas recovery (or elution) was determined by assessing the logarithmic change from the Feed to the Eluate (eqn (2)).

$$\text{Adsorption rate } (\log_{10}\text{Ads}) = \log_{10}(\text{virus in Feed}/\text{virus in Permeate}); \quad (1)$$

$$\text{Elution rate } (\log_{10}\text{Loss}) = \log_{10}(\text{virus in Feed}/\text{virus in Eluate}). \quad (2)$$

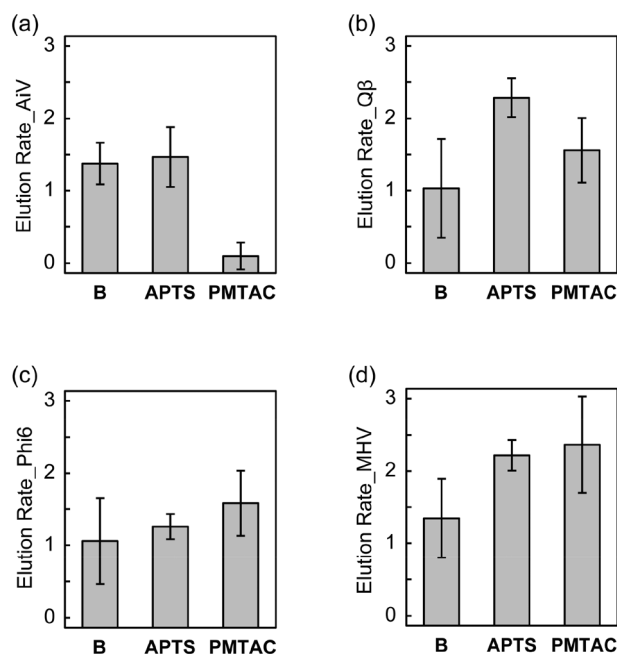


**Fig. 6** Elution rates of (a) AiV, (b) Qβ, (c) Phi6, and (d) MHV by the silicon-based substrates. Elution rate ( $\log_{10}\text{Loss}$ ) =  $\log_{10}(\text{virus in Feed}/\text{virus in Eluate})$ . **B**: bare substrates ( $n = 8$ ); **APTS**: the 3-aminopropyltriethoxysilane (APTS)-functionalized substrates ( $n = 4$ ); and **PMTAC**: the poly[2-(methacryloyloxy)ethyltrimethylammonium chloride] (PMTAC)-grafted substrates ( $n = 10$ ).

We found that the adsorption of the four tested viruses on the silicon substrates was enhanced by surface modification with the PMTAC brushes (Fig. 5). The adsorption rate of AiV by **PMTAC** increased to  $1.07 \pm 0.52 \log_{10}\text{Ads}$  (91.49% in percentage) (Fig. 5a), while those by **B** and **APTS** were  $0.13 \pm 0.11 \log_{10}\text{Ads}$  (25.11%) and  $-0.12 \pm 0.10 \log_{10}\text{Ads}$  (−33.08%), respectively (Fig. 5a). Similar trends were observed for Qβ (Fig. 5b), Phi6 (Fig. 5c), and MHV (Fig. 5d). The increase in the virus adsorption by grafting the PMTAC brushes may be due to the electrostatic interactions between the cationic polymers and the viruses.<sup>61,62</sup> It is noteworthy that the virus adsorption of **PMTAC** was higher than that of **APTS** (Fig. 5). The primary amino group of **APTS** is considered to be positively charged in the PBS solutions.<sup>63</sup> These results suggest that the cationic PMTAC brushes grafted on the substrates efficiently interact with the viruses in the aqueous phase.

The elution rates of the nonenveloped and enveloped viruses from the surface-modified and bare substrates are shown in Fig. 6, where the values of elution rates closer to zero indicate higher recovery of viruses. **PMTAC** exhibited higher recovery (elution) of AiV ( $0.10 \pm 0.18 \log_{10}\text{Loss}$ , 79.96% in percentage) than **APTS** ( $1.47 \pm 0.41 \log_{10}\text{Loss}$ , 3.42% in percentage) and **B** ( $1.38 \pm 0.29 \log_{10}\text{Loss}$ , 4.22% in percentage) (Fig. 6a). In contrast, the elution rates for Qβ (Fig. 6b), Phi6 (Fig. 6c), and MHV (Fig. 6d) rather decreased by the surface modification with the PMTAC brushes and APTS. Although the elution behavior is complicated, a combination of electrostatic

**Table 2** The average of adsorption rates ( $\log_{10}\text{Ads}$ ) and elution rates ( $\log_{10}\text{Loss}$ ) for bare and surface-modified silicon surfaces

Materials <sup>a</sup>	Viruses	Adsorption		Elution	
		Average <sup>b</sup> ( $\log_{10}\text{Ads}$ )	Average <sup>c</sup> (Ads, %)	Average <sup>b</sup> ( $\log_{10}\text{Loss}$ )	Average <sup>c</sup> (Elu, %)
<b>B</b>	AiV	0.13	25.11	1.38	4.22
	Qβ	0.55	71.97	1.03	9.33
	Phi6	0.23	41.33	1.06	8.72
	MHV	0.86	86.35	1.35	4.50
<b>APTS</b>	AiV	−0.12**	−33.08	1.47	3.42
	Qβ	0.36*	56.83	2.29***	0.52
	Phi6	0.34	54.32	1.26	5.52
	MHV	1.01	90.23	2.22**	0.61
<b>PMTAC</b>	AiV	1.07***	91.49	0.10***	79.96
	Qβ	1.66***	97.81	1.56	2.77
	Phi6	1.15***	92.94	1.58	2.61
	MHV	1.60**	97.50	2.36**	0.43

<sup>a</sup> **B**: bare substrates ( $n = 8$ ); **APTS**: 3-aminopropyltriethoxysilane (APTS)-functionalized substrates ( $n = 4$ ) and **PMTAC**: poly[2-(methacryloyloxy)ethyltrimethylammonium chloride] (PMTAC)-grafted substrates ( $n = 10$ ). <sup>b</sup> The stars indicate the significance of differences ( $p$  value) between **APTS** and **B**, **PMTAC** and **B**. \*:  $p < 0.05$ ; \*\*:  $p < 0.01$ ; and \*\*\*:  $p < 0.001$ . <sup>c</sup> The average of adsorption rates ( $\log_{10}\text{Ads}$ ) and elution rates ( $\log_{10}\text{Loss}$ ) is calculated into the form of percentage.





interactions and hydrophobic effects might result in the selective elution of AiV from the PMTAC brushes.<sup>64–66</sup>

Tables 2 and S1† summarize the average and significance of differences (*p* value) of adsorption and elution rates for the silicon-based surfaces. Statistically significant differences in virus adsorption were observed between PMTAC and B (*p* < 0.001 for AiV, Qβ, and Phi6, *p* < 0.01 for MHV). Moreover, PMTAC exhibited significantly higher elution of AiV compared to B (*p* < 0.001). Similar differences were observed between PMTAC and APTS in the virus adsorption (*p* < 0.001 for AiV, Qβ, and Phi6) and elution (*p* < 0.01 for AiV and Qβ) (Table S1†). Overall, the tuning of the virus adsorption and elution was demonstrated by using the PMTAC brushes (Fig. 1).

A plaque assay was performed to quantify Qβ as a representative infectious nonenveloped virus (Fig. 7). Comparison of the concentrations of Qβ measured by RT-qPCR and plaque assay provides insights into the inactivation of the phages.<sup>15</sup> For the feed solutions, the differences in the concentrations of Qβ observed between RT-qPCR and plaque assay were around 2 log (Fig. 7). The bare and modified substrates also exhibited

similar differences for both the Permeate (Fig. 7a) and Eluate (Fig. 7b). These results imply that the integrity of the virus particle is maintained in the adsorption and elution processes.

## Conclusions

In conclusion, we have demonstrated that the cationic PMTAC brushes enhanced not only the adsorption of enveloped and nonenveloped viruses but also the elution of AiV. The surface modification with the cationic polymers can be applied to practical virus adsorption materials with high surface area such as gauze and glass fibers. Grafting the cationic polymer brushes may provide a new direction in controlling virus adsorption and elution for passive sampling of viruses from water. The efficient adsorption and elution of target viruses may lead to precise monitoring of infectious diseases in local communities.

## Experimental

### Materials and methods

All the reagents for the preparation of the surface-modified substrates were purchased from Tokyo Chemical Industry (Tokyo, Japan), Sigma-Aldrich Japan (Tokyo, Japan), FUJIFILM Wako (Osaka, Japan), and Nacalai Tesque (Kyoto, Japan). These reagents were used as received unless otherwise stated. 2-Bromo-2-methyl-*N*-(3-(triethoxysilyl)propyl)propanamide was synthesized according to a procedure previously reported.<sup>67</sup> The surface of silicon substrates was cleaned with a FEMTO SCIENCE plasma treatment chamber CIONE4 filled with argon (80 W, 1 min) before the surface modification.

Fourier-transform infrared (FT-IR) spectra were obtained with a JASCO FT/IR-6100 Plus spectrometer and a JASCO IRT-5000 in the reflection mode. Atomic force microscopy (AFM) was performed using a Bruker MultiMode 8 atomic force microscope with a Nanoscope V controller. Contact angle measurements were performed using a Kyowa Interface Science DropMaster DMF-301 contact angle meter. The measurements were conducted at four different points for each substrate. UV-vis absorption spectroscopy was performed with a JASCO V-670 spectrophotometer.

### Preparation of the surface-modified substrates

**Poly[2-(methacryloyloxy)ethyltrimethylammonium chloride] (PMTAC)-grafted substrates.** A silicon substrate (1 cm × 1 cm) was immersed in a 11 wt% xylene solution of 2-bromo-2-methyl-*N*-(3-(triethoxysilyl)propyl)propanamide containing a drop of acetic acid for 6 h at 70 °C. The substrate was washed with ethanol and dried with a stream of argon to afford an ATRP-initiator modified substrate.

A solution of [2-(methacryloyloxy)ethyl]trimethylammonium chloride (75 wt% in H<sub>2</sub>O, 2.85 g, 10.3 mmol), methanol (2.0 mL), and deionized water (5.2 mL) was degassed by three freeze–pump–thaw cycles. *N,N,N',N',N''*-

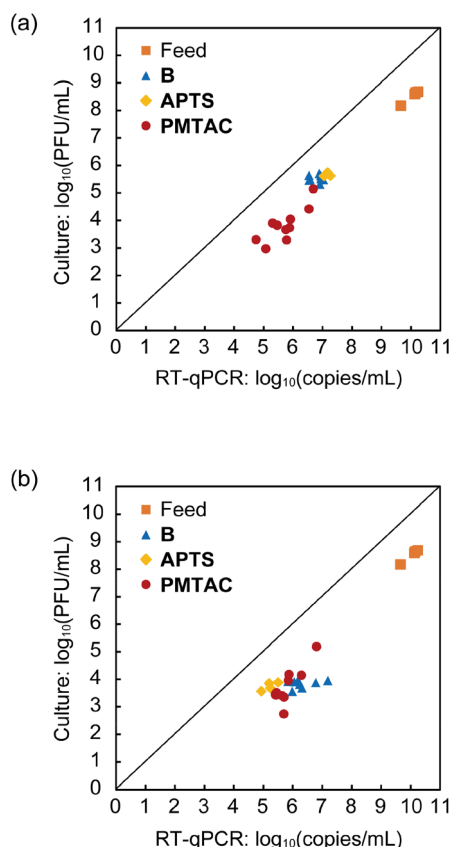


**Fig. 7** Concentrations of Qβ measured by the culture method and RT-qPCR for (a) the Permeate and (b) Eluate. Feed: the feed solutions used for the experiments; B: bare substrates; APTS: the 3-aminopropyl-triethoxysilane (APTS)-functionalized substrates; and PMTAC: the poly [2-(methacryloyloxy)ethyltrimethylammonium chloride] (PMTAC)-grafted substrates.



Pentamethyldiethylenetriamine (PMDETA) (64.6 mg, 0.37 mmol) and CuBr (12.6 mg, 0.088 mmol) were added to the deoxygenated solution under argon flow. The mixture was stirred for 5 min at 25 °C. To this mixture, the ATRP-initiator modified substrate was transferred. The mixture was stirred for 5 h at 25 °C. After removing the solution, the substrate was washed with methanol and deionized water and dried with a stream of argon to give a PMTAC-grafted substrate.

**3-Aminopropyltriethoxysilane (APTS)-functionalized substrates.** A silicon substrate (1 cm × 1 cm) was immersed in a 11 wt% xylene solution of 3-aminopropyltriethoxysilane containing a drop of acetic acid for 6 h at 70 °C. The substrate was washed with ethanol and dried with a stream of argon to give an APTS-functionalized substrate.

### Estimation of the number of solvent-accessible cations

The number of solvent-accessible cations on the PMTAC-grafted, APTS-functionalized, and nonmodified bare substrates was estimated by a fluorescein adsorption assay according to procedures reported previously.<sup>53,54</sup> The substrates with a total surface area of 2 cm<sup>2</sup> were immersed in 1 wt% aqueous solution of sodium fluorescein (10 mL) for 20 min under gentle shaking. These substrates were washed with deionized water and placed in water (10 mL) with ultrasonication for 10 min. This washing process was repeated three times. To desorb the immobilized fluorescein, the substrates were immersed in a 0.1 wt% aqueous solution of cetyltrimethylammonium chloride (9 mL) for 30 min under gentle shaking. 0.1 M PBS buffer (pH 8.0) (1 mL) was added to the solution after the removal of the substrates. The absorbance of the solution at 501 nm was measured. The concentration of the desorbed fluorescein was estimated based on Beer-Lambert law with the extinction coefficient of fluorescein of 77 000 M<sup>-1</sup> cm<sup>-1</sup>, and an optical path length of 1 cm. The number of solvent-accessible cations on the substrates can be correlated with the concentration of fluorescein by assuming a 1:1 complexation of fluorescein with the cationic group. These measurements were performed three times for each substrate.

### Virus preparation

Phi6 and MHV were used as surrogates to represent enveloped viruses, whereas Qβ and AiV were used for non-enveloped viruses. Bacteriophage Phi6 (NBRC 105899, National Institute of Technology and Evaluation, Tokyo, Japan) was propagated using *P. syringae* (NBRC14084, NITE) as the host bacterium according to the protocol. Bacteriophage Qβ (ATCC23631-B1, the American Type Culture Collection, Manassas, Virginia, USA) was propagated in the lab using *Escherichia coli* K12 A/λ F<sup>+</sup> as the host bacteria.<sup>68</sup> The AiV strain (strain A846/88 donated by Dr Yamashita from Shubun University, Aichi, Japan) and MHV A59 strain (ATCC VR-764) were propagated using buffalo green monkey kidney cells and DBT cells, respectively, as described before.<sup>69,70</sup> Host cells were removed by centrifugation at 3000 rpm for 10 min followed by membrane filtration with a cellulose acetate filter (0.2 μm, DISMIC-25CS, Advantec, Tokyo, Japan). Then the viruses were

further purified by gel filtration with an Illustra Microspin S-300 HR column (GE Healthcare, Tokyo, Japan).<sup>71,72</sup> The purified viruses were quantified by RT-qPCR (MHV, AiV, Qβ and Phi6) and plaque assay (Qβ), aliquoted and stored at -80 °C until being used as intact virus stock. For each experiment, the 4 types of viruses were mixed into 1 mL of 100 mM PBS to make the feed solution (Feed) at the initial concentrations of 10<sup>8</sup> PFU mL<sup>-1</sup> for Qβ, and 10<sub>9</sub> – 10<sub>10</sub> copies per mL for AiV, Qβ, Phi6, and MHV.

### Virus adsorption and elution

A 5 μL feed solution was dropped onto a test substrate (1 cm × 1 cm) in a Petri dish. A cover glass was placed on top of the substrate. After incubation at 25 °C for 5 h, the substrate was washed with 100 mM PBS (2.5 mL). The solution was collected as the permeate (referred to as Permeate).

The substrate used for virus adsorption was transferred to a 12-well cell culture plate and soaked in 2.5 mL of sterile beef extract (3%, pH = 9). After incubation at 25 °C for 1 h, the solution was collected as the eluate (referred to as Eluate). Throughout the experiments, the Feed, Permeate, and Eluate samples were stored at 4 °C until further analysis within 24 h. Successive treatment of adsorption and elution was performed for each test substrate.

### Quantification of viruses

The concentrations of all the tested viruses in the Feed, Permeate, and Eluate were determined using reverse transcription quantitative polymerase chain reaction (RT-qPCR). Initially, RNA was extracted from 140 μL of each sample utilizing a QIAamp Viral RNA Mini Kit (Qiagen, Hilden, Germany). Subsequently, reverse transcription was performed using a High-Capacity cDNA Reverse Transcription Kit with an RNase Inhibitor (Applied Biosystems, USA). The resulting cDNA products were subjected to qPCR analysis. For the qPCR, a 25 μL reaction mixture was prepared, comprising 12.5 μL of TaqMan<sup>TM</sup> Gene Expression Master Mix (Applied Biosystems), 1 μL of forward and reverse primers (10 μmol L<sup>-1</sup>), 0.5 μL of TaqMan probes (5 μmol L<sup>-1</sup>), and 5 μL of cDNA. The primers for Qβ,<sup>73</sup> Phi6,<sup>74</sup> AiV,<sup>75</sup> and MHV<sup>76</sup> were prepared according to the literature. RT-qPCR was carried out in duplicate on an ABI StepOnePlus thermocycler (Thermo Fisher, USA), following the recommended temperature conditions outlined in the previous studies, which varied depending on the virus type. For each 96-well RT-qPCR plate, negative controls were performed with sterile water. Standard curves were generated using 10-fold serial dilutions of pre-determined plasmid DNA containing the target gene sequence, covering target virus concentrations ranging from 10<sup>6</sup> to 10<sup>0</sup> copies per reaction. The amplification efficiencies exceeded 90% and the correlation factor (*R*<sup>2</sup>) was higher than 0.99. The assay limit of detection was 2 copy per μL (10 copy per reaction) for all the tested viruses. The process limit of detection was 1720 copies per mL sample.<sup>77</sup>

In order to assess the adsorption and elution rates of infectious viruses in passive sampling, a plaque assay was con-



ducted for the bacteriophage Q $\beta$ . To perform the assay, the Feed, Permeate, and Eluate samples were subjected to serial 10-fold dilution and plated onto LB agar plates pre-inoculated with host bacteria, specifically *E. coli* K12 F<sup>+</sup> (A/ $\lambda$ ). Duplicate plates were prepared for each sample at every dilution level. The plates were then incubated at 37 °C overnight to allow the formation of visible plaques, which were subsequently counted for analysis.

## Author contributions

T. K. and H. K. conceived and designed the project. J. U., M. L., and S. M. performed the experiments and data analysis. J. U. and T. K. wrote the manuscript. All authors read and commented on the manuscript.

## Conflicts of interest

There are no conflicts to declare.

## Acknowledgements

This work was supported by JST, CREST Grant Number JPMJCR20H3 and JSPS KAKENHI Grant Number JP19H05715 (Grant-in-Aid for Scientific Research on Innovative Area: Aquatic Functional Materials). We greatly appreciate Harumi Ishikawa, Terumi Seya, Miwako Nakagawa, and Dr Tippawan Singhonpon for their valuable support in the experiments.

## References

- 1 M. Kitajima, W. Ahmed, K. Bibby, A. Carducci, C. P. Gerba, K. A. Hamilton, E. Haramoto and J. B. Rose, *Sci. Total Environ.*, 2020, **739**, 139076.
- 2 A. C. Singer, J. R. Thompson, C. R. M. Filho, R. Street, X. Li, S. Castiglioni and K. V. Thomas, *Nat. Water*, 2023, **1**, 408–415.
- 3 K. M. S. de Melo Cassemiro, F. M. Burlandy, M. R. F. Barbosa, Q. Chen, J. Jorba, E. M. Hachich, M. I. Z. Sato, C. C. Burns and E. E. da Silva, *PLoS One*, 2016, **11**, e0152251.
- 4 J. Habtewold, D. McCarthy, E. McBean, I. Law, L. Goodridge, M. Habash and H. M. Murphy, *Environ. Res.*, 2022, **204**, 112058.
- 5 M. Kitajima, M. Murakami, R. Iwamoto, H. Katayama and S. Imoto, *J. Travel Med.*, 2022, **29**, taac004.
- 6 M. Kitajima and C. P. Gerba, *Pathogens*, 2015, **4**, 256–268.
- 7 F. S. Le Guyader, J.-C. Le Saux, K. Ambert-Balay, J. Krol, O. Serais, S. Parnaudeau, H. Giraudon, G. Delmas, M. Pommepuy, P. Pothier and R. L. Atmar, *J. Clin. Microbiol.*, 2008, **46**, 4011–4017.
- 8 K. Sdiri-Loulizi, M. Hassine, Z. Aouni, H. Gharbi-Khelifi, N. Sakly, S. Chouchane, M. Guediche, P. Pothier, M. Aouni and K. Ambert-Balay, *Arch. Virol.*, 2010, **155**, 1509–1513.
- 9 M. Kitajima, B. C. Iker, I. L. Pepper and C. P. Gerba, *Sci. Total Environ.*, 2014, **488–489**, 290–296.
- 10 G. Matrajt, B. Naughton, A. S. Bandyopadhyay and J. S. Meschke, *Clin. Infect. Dis.*, 2018, **67**, S90–S97.
- 11 C. Schang, N. D. Crosbie, M. Nolan, R. Poon, M. Wang, A. Jex, N. John, L. Baker, P. Scales, J. Schmidt, B. R. Thorley, K. Hill, A. Zamyadi, C.-W. Tseng, R. Henry, P. Kolotelo, J. Langeveld, R. Schilperoort, B. Shi, S. Einsiedel, M. Thomas, J. Black, S. Wilson and D. T. McCarthy, *Environ. Sci. Technol.*, 2021, **55**, 10432–10441.
- 12 B. Moore, *Mon. Bull. Minist. Health Public Health Lab. Serv.*, 1948, **7**, 241–248.
- 13 J. Voisin, B. Cournoyer and F. Mermillod-Blondin, *Houille Blanche*, 2015, **4**, 52–57.
- 14 F. Vincent-Hubert, B. Morga, T. Renault and F. Le Guyader, *J. Appl. Microbiol.*, 2017, **122**, 1039–1047.
- 15 M. Liu, J. Uchida, S. Matsuyama, T. Kato and H. Katayama, *ACS ES&T Water*, 2024, **4**, 368–376.
- 16 J. O. Zoppe, N. C. Ataman, P. Mocny, J. Wang, J. Moraes and H.-A. Klok, *Chem. Rev.*, 2017, **117**, 1105–1318.
- 17 Y. Tsujii, K. Ohno, S. Yamamoto, A. Goto and T. Fukuda, *Adv. Polym. Sci.*, 2006, **197**, 1–45.
- 18 Y. Higaki, M. Kobayashi, D. Murakami and A. Takahara, *Polym. J.*, 2016, **48**, 325–331.
- 19 T. Masuda and M. Takai, *J. Mater. Chem. B*, 2022, **10**, 1473–1485.
- 20 M. Ejaz, S. Yamamoto, K. Ohno, Y. Tsujii and T. Fukuda, *Macromolecules*, 1998, **31**, 5934–5936.
- 21 T. von Werne and T. E. Patten, *J. Am. Chem. Soc.*, 1999, **121**, 7409–7410.
- 22 M. Kohri, *Polym. J.*, 2019, **51**, 1127–1135.
- 23 Y. Takeoka, *Polym. J.*, 2015, **47**, 106–113.
- 24 H. Arafune, T. Kamijo, T. Morinaga, S. Honma, T. Sato and Y. Tsujii, *Adv. Mater. Interfaces*, 2015, **2**, 1500187.
- 25 K. Kitano, Y. Inoue, R. Matsuno, M. Takai and K. Ishihara, *Colloids Surf., B*, 2009, **74**, 350–357.
- 26 U. Raviv, S. Giasson, N. Kampf, J.-F. Gohy, R. Jérôme and J. Klein, *Nature*, 2003, **425**, 163–165.
- 27 M. Kobayashi, Y. Terayama, H. Yamaguchi, M. Terada, D. Murakami, K. Ishihara and A. Takahara, *Langmuir*, 2012, **28**, 7212–7222.
- 28 J. B. Schlenoff, *Langmuir*, 2014, **30**, 9625–9636.
- 29 M. Krishnamoorthy, S. Hakobyan, M. Ramstedt and J. E. Gautrot, *Chem. Rev.*, 2014, **114**, 10976–11026.
- 30 N. Hadjesfandiari, K. Yu, Y. Mei and J. N. Kizhakkedathu, *J. Mater. Chem. B*, 2014, **2**, 4968–4978.
- 31 T. Shimizu, M. Yamato, A. Kikuchi and T. Okano, *Biomaterials*, 2003, **24**, 2309–2316.
- 32 Y. G. Takei, T. Aoki, K. Sanui, N. Ogata, Y. Sakurai and T. Okano, *Macromolecules*, 1994, **27**, 6163–6166.
- 33 S. Kumar, T. Ito, Y. Yanagihara, Y. Oaki, T. Nishimura and T. Kato, *CrystEngComm*, 2010, **12**, 2021–2024.



- 34 Y. Han, T. Nishimura and T. Kato, *Polym. J.*, 2014, **46**, 499–504.
- 35 Y. Han, T. Nishimura and T. Kato, *CrystEngComm*, 2014, **16**, 3540–3547.
- 36 B. Michen and T. Graule, *J. Appl. Microbiol.*, 2010, **109**, 388–397.
- 37 M. D. Sobsey and B. L. Jones, *Appl. Environ. Microbiol.*, 1979, **37**, 588–595.
- 38 N. Marets, D. Kuo, J. R. Torrey, T. Sakamoto, M. Henmi, H. Katayama and T. Kato, *Adv. Healthcare Mater.*, 2017, **6**, 1700252.
- 39 K. Hamaguchi, R. Ichikawa, S. Kajiyama, S. Torii, Y. Hayashi, J. Kumaki, H. Katayama and T. Kato, *ACS Appl. Mater. Interfaces*, 2021, **13**, 20598–20605.
- 40 D. Kuo, M. Liu, K. R. S. Kumar, K. Hamaguchi, K. P. Gan, T. Sakamoto, T. Ogawa, R. Kato, N. Miyamoto, H. Nada, M. Kimura, M. Henmi, H. Katayama and T. Kato, *Small*, 2020, **16**, 2001721.
- 41 D. Kuo, T. Sakamoto, S. Torii, M. Liu, H. Katayama and T. Kato, *Polym. J.*, 2022, **54**, 821–825.
- 42 T. Sakamoto, K. Asakura, N. Kang, R. Kato, M. Liu, T. Hayashi, H. Katayama and T. Kato, *J. Mater. Chem. A*, 2023, **11**, 22178–22186.
- 43 K. Fukushima, K. Kishi, K. Saito, K. Takakuwa, S. Hakozaiki and S. Yano, *Biomater. Sci.*, 2019, **7**, 2288–2296.
- 44 K. Lienkamp, A. E. Madkour, A. Musante, C. F. Nelson, K. Nüsslein and G. N. Tew, *J. Am. Chem. Soc.*, 2008, **130**(30), 9836–9843.
- 45 F. Nederberg, Y. Zhang, J. P. K. Tan, K. Xu, H. Wang, C. Yang, S. Gao, X. D. Guo, K. Fukushima, L. Li, J. L. Hedrick and Y.-Y. Yang, *Nat. Chem.*, 2011, **3**, 409–414.
- 46 K. Nagase, S. Kitazawa, T. Kogure, S. Yamada, K. Katayama and H. Kanazawa, *Sep. Purif. Technol.*, 2022, **286**, 120445.
- 47 K. Matyjaszewski and J. H. Xia, *Chem. Rev.*, 2001, **101**, 2921–2990.
- 48 J. Pyun and K. Matyjaszewski, *Chem. Mater.*, 2001, **13**, 3436–3448.
- 49 M. Kobayashi and A. Takahara, *Chem. Rec.*, 2010, **10**, 208–216.
- 50 K. Gao, Y. Su, L. Zhou, M. He, R. Zhang, Y. Liu and Z. Jiang, *J. Membr. Sci.*, 2018, **548**, 621–631.
- 51 S. L. Banerjee, T. Swift, R. Hoskins, S. Rimmer and N. K. Singha, *J. Mater. Chem. B*, 2019, **7**, 1475–1493.
- 52 K. Koch, B. Bhushan and W. Barthlott, *Soft Matter*, 2008, **4**, 1943–1963.
- 53 J. C. Tiller, C. J. Liao, K. Lewis and A. M. Klibanov, *Proc. Natl. Acad. Sci. U. S. A.*, 2001, **98**, 5981–5985.
- 54 E. Zorn, J. I. H. Knaack, N. Burmeister, N. Scharnagl, M. Rohnke, S. G. Wicha and W. Maison, *Langmuir*, 2023, **39**, 11063–11072.
- 55 N. Shirasaki, T. Matsushita, Y. Matsui, T. Urasaki and K. Ohno, *Water Res.*, 2009, **43**, 605–612.
- 56 J. Langlet, L. Ogorzaly, J.-C. Schrotter, C. Machinal, F. Gaboriaud, J. F. L. Duval and C. Gantzer, *J. Membr. Sci.*, 2009, **326**, 111–116.
- 57 T. Yamashita, S. Kobayashi, K. Sakae, S. Nakata, S. Chiba, Y. Ishihara and S. Isomura, *J. Infect. Dis.*, 1991, **164**, 954–957.
- 58 M. Bárcena, G. T. Oostergetel, W. Bartelink, F. G. A. Faas, A. Verkleij, P. J. M. Rottier, A. J. Koster and B. J. Bosch, *Proc. Natl. Acad. Sci. U. S. A.*, 2009, **106**, 582–587.
- 59 A. Katz, S. Peña, A. Alimova, P. Gottlieb, M. Xu and K. A. Block, *Sci. Total Environ.*, 2018, **637–638**, 104–111.
- 60 K. J. Schwab, R. D. Leon and M. D. Sobsey, *Appl. Environ. Microbiol.*, 1995, **61**, 531–537.
- 61 M. D. Sobsey and B. L. Jones, *Appl. Environ. Microbiol.*, 1979, **37**, 588–595.
- 62 R. Attinti, J. Wei, K. Kniel, J. T. Sims and Y. Jin, *Environ. Sci. Technol.*, 2010, **44**, 2426–2432.
- 63 J. Liu, H. Zhang, D. Xue, A. ul Ahmad, X. Xia, Y. Liu, H. Huang, W. Guo and H. Liang, *RSC Adv.*, 2020, **10**, 11393–11399.
- 64 C. P. Gerba, *Adv. Appl. Microbiol.*, 1984, **30**, 133–168.
- 65 A. Armanious, M. Aeppli, R. Jacak, D. Refardt, T. Sigstam, T. Kohn and M. Sander, *Environ. Sci. Technol.*, 2016, **50**, 732–743.
- 66 J. Langlet, F. Gaboriaud, J. F. L. Duval and C. Gantzer, *Water Res.*, 2008, **42**, 2769–2777.
- 67 M. J. Mulvihill, B. L. Rupert, R. He, A. Hochbaum, J. Arnold and P. Yang, *J. Am. Chem. Soc.*, 2005, **127**, 16040–16041.
- 68 R. Kato, T. Asami, E. Utagawa, H. Furumai and H. Katayama, *Water Res.*, 2018, **132**, 61–70.
- 69 V. D. Canh, I. Kasuga, H. Furumai and H. Katayama, *Food Environ. Virol.*, 2019, **11**, 40–51.
- 70 V. D. Canh, S. Torii, H. Furumai and H. Katayama, *Water Res.*, 2021, **189**, 116674.
- 71 M. Kitajima, T. Oka, E. Haramoto, H. Katayama, N. Takeda, K. Katayama and S. Ohgaki, *Appl. Environ. Microbiol.*, 2010, **76**, 2461–2467.
- 72 M. Kitajima, T. Oka, E. Haramoto, N. Takeda, K. Katayama and H. Katayama, *Environ. Sci. Technol.*, 2010, **44**, 7116–7122.
- 73 S. Wolf, J. Hewitt and G. E. Greening, *Appl. Environ. Microbiol.*, 2010, **76**, 1388–1394.
- 74 L. Gendron, D. Verreault, M. Veillette, S. Moineau and C. Duchaine, *Aerosol Sci. Technol.*, 2010, **44**, 893–901.
- 75 M. Kitajima, A. Hata, T. Yamashita, E. Haramoto, H. Minagawa and H. Katayama, *Appl. Environ. Microbiol.*, 2013, **79**, 3952–3958.
- 76 G. D. Smith, P. J. Solenberg, M. C. Koenig, K. A. Brune and N. Fox, *Comp. Med.*, 2002, **52**, 456–460.
- 77 W. Ahmed, A. Bivins, S. Metcalfe, W. J. Smith, M. E. Verbyla, E. M. Symonds and S. L. Simpson, *Water Res.*, 2022, **213**, 118132.

